



**ME 699: Magnetohydrodynamics and its Engineering  
Applications**

---

**MHD DRAG REDUCTION IN TURBULENT FLOWS  
OF POORLY CONDUCTING FLUID**

---

M Vishnu Sankar - 18B030013

Course Instructor : Prof. Avishek Ranjan

Indian Institute of Technology, Bombay

# Contents

|          |   |           |
|----------|---|-----------|
| <b>1</b> | <b>Introduction and Motivation</b>                | <b>1</b>  |
| <b>2</b> | <b>Literature Review and Previous Work</b>        | <b>2</b>  |
| <b>3</b> | <b>Governing Equations and Problem Set-up</b>     | <b>4</b>  |
| 3.1      | Flow in a channel . . . . .                       | 4         |
| 3.2      | Low MHD Approximation . . . . .                   | 5         |
| 3.3      | Results . . . . .                                 | 6         |
| 3.4      | Grid Independence Test . . . . .                  | 7         |
| 3.5      | Flow field at different Reynolds number . . . . . | 8         |
| 3.6      | Turbulent Flow around a Cylinder . . . . .        | 9         |
| 3.6.1    | Geometry and Mesh . . . . .                       | 9         |
| 3.6.2    | Boundary Condition . . . . .                      | 10        |
| 3.7      | Flow beyond a Backward Step . . . . .             | 11        |
| 3.7.1    | Geometry . . . . .                                | 11        |
| <b>4</b> | <b>Results &amp; Discussion</b>                   | <b>13</b> |
| 4.1      | Case 1: Without Lorentz Force . . . . .           | 13        |
| 4.2      | Case 2 and 3: With Lorentz Force . . . . .        | 14        |
| 4.2.1    | Comparing Eddy Viscosity . . . . .                | 15        |
| 4.2.2    | Circumferential Velocity . . . . .                | 16        |
| 4.2.3    | Velocity Deficit . . . . .                        | 17        |
| 4.3      | Conclusion for Flow Over Cylinder . . . . .       | 20        |
| 4.4      | Results for Flow beyond a Backward Step . . . . . | 21        |
| <b>5</b> | <b>REFERENCES</b>                                 | <b>24</b> |

---

# 1 Introduction and Motivation

Drag reduction through flow control is a central issue for fluid dynamisicist and engineers, not just because it can save lots of fuel and money but also due to the fact that the area of active flow control has become very interdisciplinary in nature which continues to attract many people over the last few decades.

Flow control can be achieved though passive or active methods. Passive methods usually include moving or non-moving mechanical parts such as vortex generators, or flow vanes, leading-edge serrations. But such passive methods do not give a control authority over the flow. On the other hand Active flow control methods give a high control authority over the flow. Some examples are Di-electric barrier discharge actuators for low speed control, surface morphing using piezo-electric actuators and there has also been studies using MHD actuators which induce lorentz force. Here in my course project, I have tried to dig deeper regarding the MHD flow control in poorly conducting flows such as seawater and it has three aspects to it.

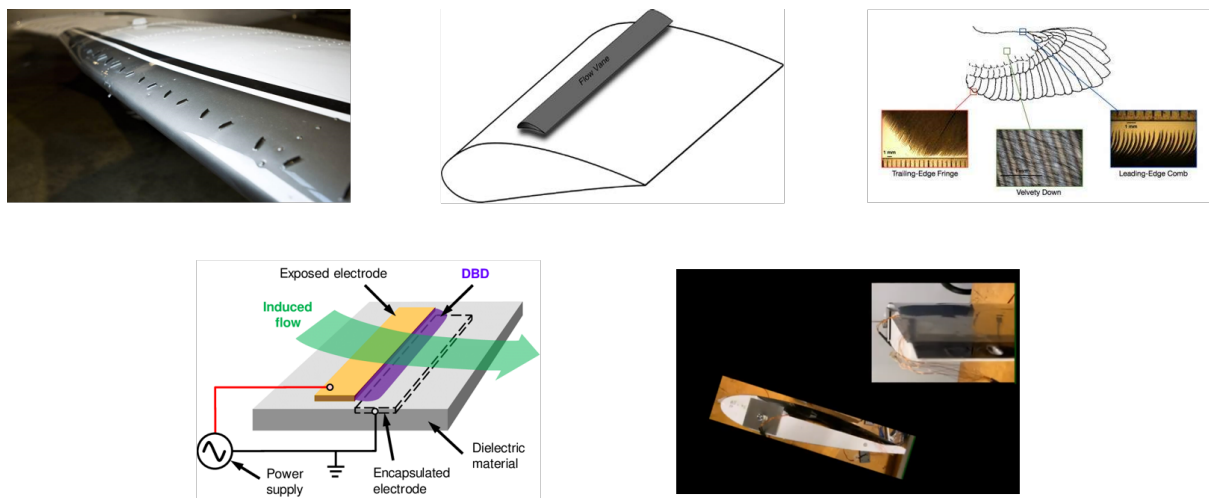


**Figure 1:** Flow control methods

---

## 2 Literature Review and Previous Work

There are three aspects of flow control<sup>[2]</sup>

- Reduce the turbulent drag by suppressing turbulence or by laminarizing the turbulent flow
- Delay transition by active wave cancellation or other techniques
- To control separated flows and shear layers

In this study I have picked up three problem statements corresponding to the first and last aspects shown above to test the effect of Lorentz force on the drag reduction and reducing flow separation.

Researchers have tried different configurations of magnets in order to study the influence of the orientation of magnetic field on the boundary layer. The first one is the tile configuration which induces a normal force and the second one is called the stripe configuration which induces a stream-wise or span-wise lorentz force.

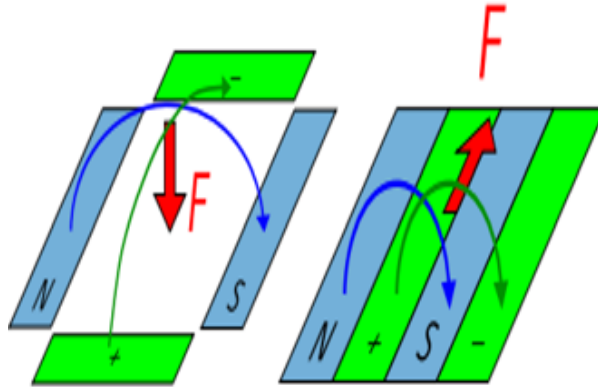


**Figure 2:** tile configuration, originally published in [2]

In a fluid with electrical conductivity  $\sigma > 0$  the current density is given by

$$J = \sigma(E + u \times B)$$

and lorentz force is given by

$$F_L = J \times B$$

---

For poorly conducting fluids like sea water,  $\sigma \approx 10$  the force may not be that significant until velocity or magnetic field is sufficiently large. While traditional flow control techniques try to change the flow dynamics just by modifying the boundary conditions, the lorentz force changes the flow physics itself by introducing a body term in the Navier-Stokes equation<sup>[2]</sup>.

Various numerical and experimental studies have been performed in the past for employing MHD flow control. Computational studies show turbulent drag reduction upto 70% [2]. But this was only for small laboratory scale level, while experimentally only 5-10% could be reported due to various challenges<sup>[2]</sup>. Various studies were conducted to study the effect of magnetic field applied along streamwise, spanwise and normal to wall direction. The results were strongly dependent on **interaction parameter**. Both spanwise and streamwise lorentz forces gave similar results, i.e upto a 40% turbulent skin-friction was reduced. Numerical studies have shown that it is indeed possible to reduce the skin friction drag by 40%, for a similar experimental set-up only upto 10% reduction could be achieved due to various practical problems. Although turbulent skin friction is reduced, in experiments this comes with a cost, and the prize to be paid is loss of efficiency. The power needed to reduce the turbulent skin friction is much more that the power that could have been lost due to turbulence. Nevertheless, in this course project the reduction of turbulent skin friction is studied for different geometries.

---

### 3 Governing Equations and Problem Set-up

Since in most of the real life aerodynamic applications flow tends to become turbulent, in all the simulations Reynolds number corresponding to turbulent flow was chosen. The conductivity of sea water is just about  $10\text{S}/\text{m}$  hence, the Magnetic Reynolds number is very low ( $O(-4)$ ). Hence all the low MHD approximations hold true.

$$\mathbf{J} = \sigma(\mathbf{E} + \mathbf{u} \times \mathbf{B})$$

$$\nabla \times \mathbf{B} = \mu_0 \mathbf{J}$$

$$\nabla \cdot \mathbf{B} = 0$$

$$\frac{\partial \mathbf{u}}{\partial t} + (\mathbf{u} \cdot \nabla) \mathbf{u} = -\frac{\nabla P}{\rho} + \frac{\mathbf{J} \times \mathbf{B}}{\rho}$$

$$\frac{\partial \mathbf{B}}{\partial t} + (\mathbf{u} \cdot \nabla) \mathbf{B} = \frac{\nabla^2 \mathbf{B}}{\mu \sigma} + (\mathbf{B} \cdot \nabla) \mathbf{u}$$

$$\frac{\partial u}{\partial x} + \frac{\partial v}{\partial y} = 0$$

Assuming the flow to be incompressible

#### 3.1 Flow in a channel

Here the flow is taken to be turbulent as the Reynolds number is already about 5000

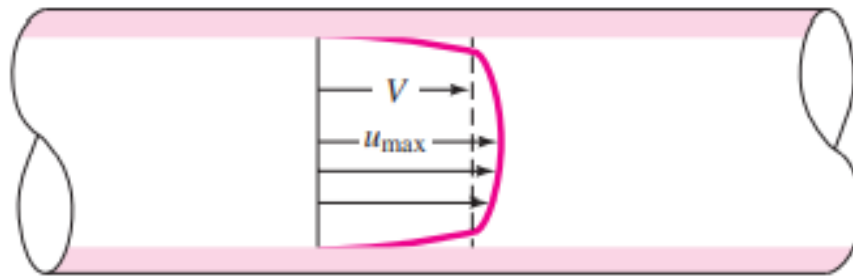


**Figure 3:** Turbulent Flow Velocity Profile inside a pipe, Originally published in [6]

### 3.2 Low MHD Approximation

So the first step was to simulate a bench mark problem that was found in the literature study. The physics of the problem is that there is a duct such that streamwise direction is the X-direction. Magnetic field is applied in the Y direction and it is observed that the velocity profile in Y direction and Z direction are different from each other. This is because in a duct flow there are 2 kinds of boundary layers, the BL perpendicular to the MF is the Hartmann BL and the BL parallel to the MF is the sidewall layer. The Hartmann layer is proportional to  $Ha^{-1}$  and the sidewall is proportional to  $Ha^{-1/2}$ . Therefore, the Hartmann layer is thinner than the sidewall layer, due to this the velocity gradients are higher and the wall shear stress and skin friction coefficient increases.

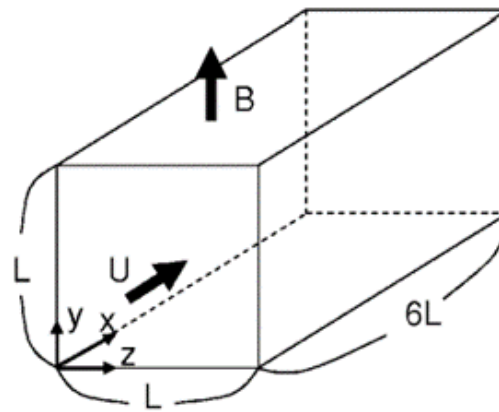
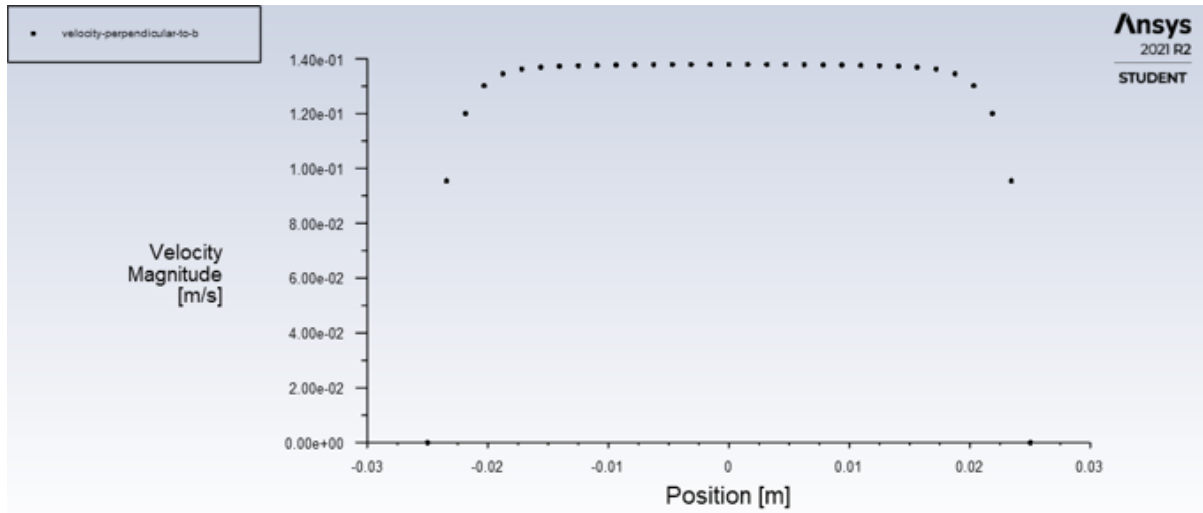


**Figure 4:** Geometry of channel

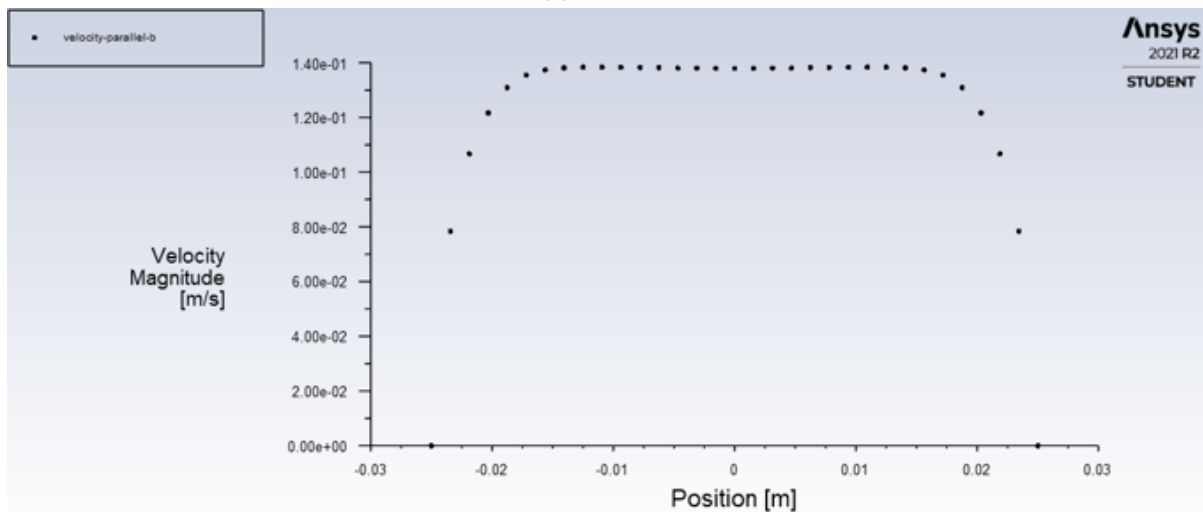
| Parameters               | Values                |
|--------------------------|-----------------------|
| $Re$                     | 5300                  |
| Density                  | 998 kg/m <sup>3</sup> |
| Conductivity             | 5 S/m                 |
| cell length              | 1.5625 mm             |
| Total Elements           | 3,25,000+             |
| Min and Max Aspect Ratio | 1                     |
| Skewness                 | $10^{-4}$             |

**Table 1:** Mesh Metrics

### 3.3 Results



(a) Side Wall



(b) Top Wall

**Figure 5:** Velocity profile perpendicular flow direction

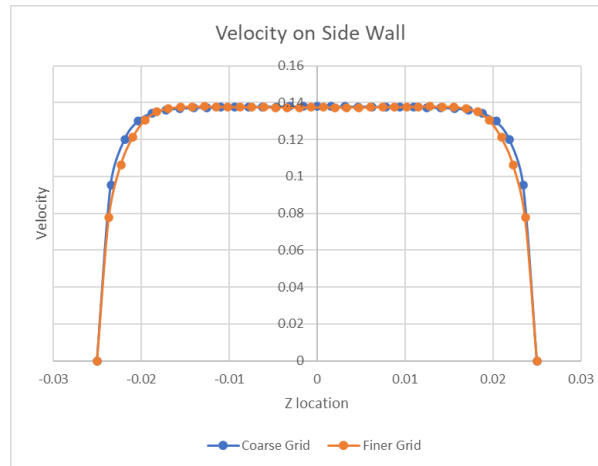
|                   | B = 0          | B = 10.5 T (Coarse Mesh) | B = 10.5 T (Fine mesh) |
|-------------------|----------------|--------------------------|------------------------|
| Drag on Top wall  | 0.0021676667 N | 0.0027234054 N           | 0.0027482179 N         |
| Drag on Side wall | 0.0021676667 N | 0.0021538442 N           | 0.0021181654 N         |



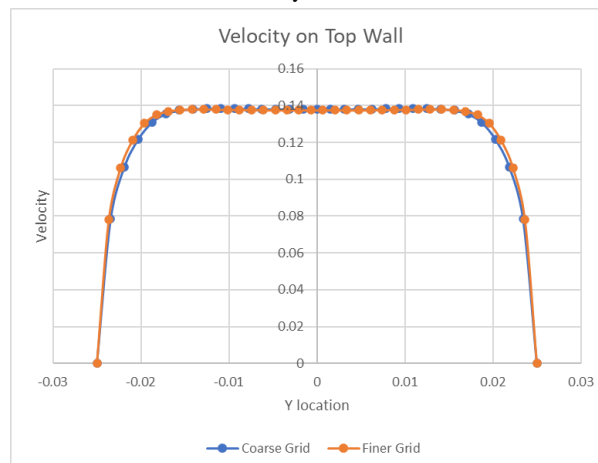
---

### 3.4 Grid Independence Test

Another grid with about 5,00,000+ elements was generated with each cubic cell having a length of 0.135 units. This was used to test if the velocity results












(a) Velocity on side wall



(b) Velocity on top wall

**Figure 6:** Velocity comparison between coarse and fine mesh

### 3.5 Flow field at different Reynolds number

| Image   | Description                         | $Re$  |
|---|-------------------------------------|---|
|    | No separation, creeping flow        | $Re < 5$  |
|    | Pair of symmetric vortices          | $5 < Re < 40$   |
|    | Laminar vortex sheet                | $40 < Re < 200$   |
|    | Transition to turbulent in the wake | $200 < Re < 300$  |
|   | Completely turbulent wake           | $300 < Re < 3 \times 10^5$ Subcritical                  |
|  | Laminar and turbulent separation    | $3 \times 10^5 < Re < 3.5 \times 10^5$ Critical         |
|  | Turbulent Separation                | $3.5 \times 10^5 < Re < 1.5 \times 10^6$ Supercritical  |
|  | Turbulent BL at one side            | $1.5 \times 10^6 < Re < 4 \times 10^6$ Upper transition |
|  | Turbulent BL at both sides          | $4 \times 10^6 < Re$ Transcritical                      |

**Table 2:** Flow at different  $Re$ , Originally published in [7]

---

### 3.6 Turbulent Flow around a Cylinder

As mentioned earlier we are interested in reducing drag due to turbulent skin friction. Here a turbulent flow around a cylinder is simulated using  $SST - k - \omega$  model as it can handle separated flows better than other turbulent models. The reynolds number is defined as

$$Re = \frac{Du_{\infty}}{\nu}$$

for this case it is about 5000 and the wake is completely turbulent as indicated by the table above.

| Parameters                  | Values    |
|-----------------------------|-----------|
| <b>Total Elements</b>       | 5,12,000+ |
| <b>Average Aspect Ratio</b> | 8         |
| <b>Skewness</b>             | $10^{-1}$ |

**Table 3:** Mesh Metrics

| Parameters        | Values                                      |
|-------------------|---|
| $u_{\infty}$      | 5 cm/s                                      |
| Diameter          | 0.1 m                                       |
| Conductivity      | 10 S/m                                      |
| $B_0$             | 5 Tesla                                     |
| cell length       | 5 mm  |
| Dynamic Viscosity | $0.001003 \text{ kg m}^{-1} \text{ s}^{-1}$ |
| Reynolds Number   | 4975  |

**Table 4:** Flow Parameters

#### 3.6.1 Geometry and Mesh

A cylinder of 10 cm diameter is enclosed in a rectangular domain of 150 cm  $\times$  75 cm.

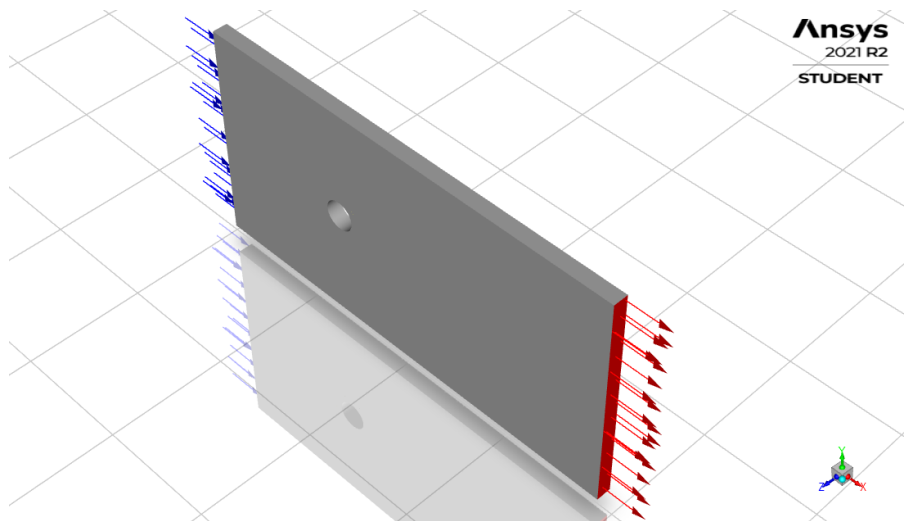


**Figure 7:** Cylinder geometry

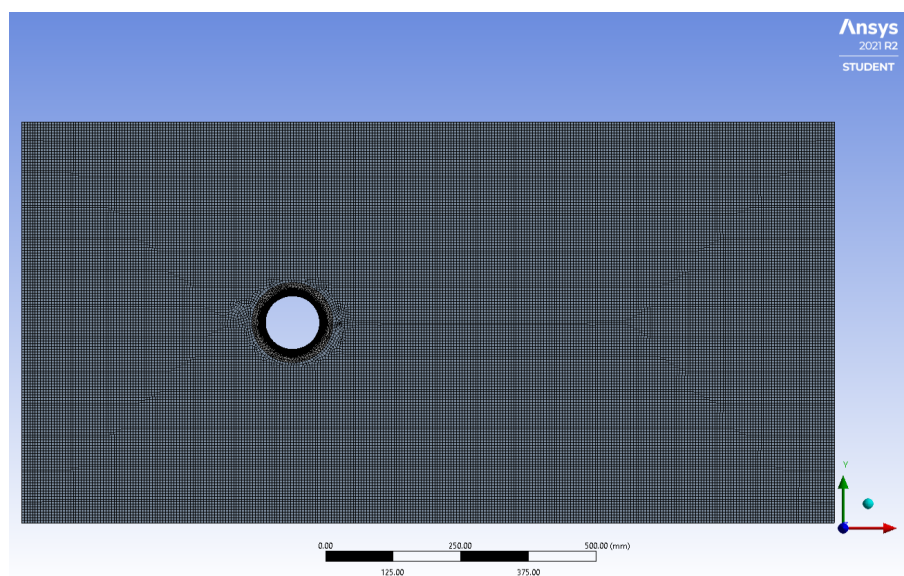


**Figure 8:** Mesh

### 3.6.2 Boundary Condition

The top wall, bottom wall, front and back wall have slip conditions. The one on the left is inlet and one on the right is the outlet. Only the surface of the cylinder is given no slip condition. For the case with Lorentz force the wall is insulated and magnetic flux cannot pass through it and hence specified magnetic flux of zero is assigned.

For a typical non-separated flow, the wake profile looks similar to the image shown below. But for a separated flow, the velocity gradient rapidly reaches close to zero and increase once

again till the center line (refer figure 17, 18 to see this). In order to find the exact location the velocity on the surface of the cylinder can be plotted or an even accurate value is provided by a zero wall shear stress on the surface of the cylinder.

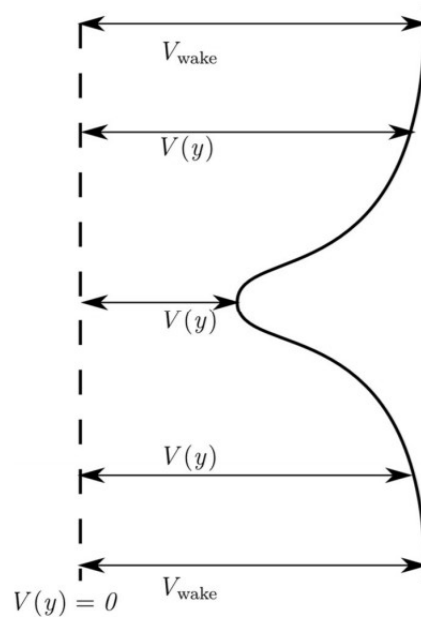


**Figure 9:** Wake Profile for non-separated flow, Originally published in [5]

### 3.7 Flow beyond a Backward Step

In aerodynamics, flow over a backward step is used to check the robustness of an algorithm by finding the separation point due to the algorithm by comparing with the experiment results. Here in this study I have tried to analyze the change in the location of separation point due to the presence of magnetic field.

#### 3.7.1 Geometry

The inlet is 5 cm in height, the location of the step is 50 cm from the inlet. There is a discontinuity in the bottom wall at the step, which has a downward height of 10 cm. The outlet is 10 cm in height. The horizontal distance between the step and the outlet is 100 cm. There are about 2,00,000 elements and it is a 2-D simulation.

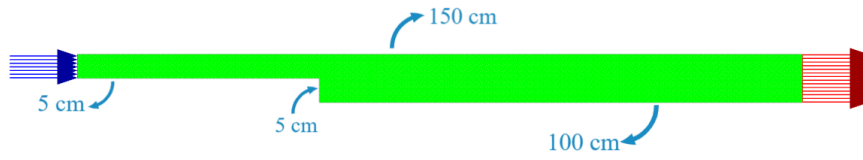


**Figure 10:** Step Geometry

Except the inlet and the outlet the remaining walls have no slip boundary conditions.

---

## 4 Results & Discussion

### 4.1 Case 1: Without Lorentz Force

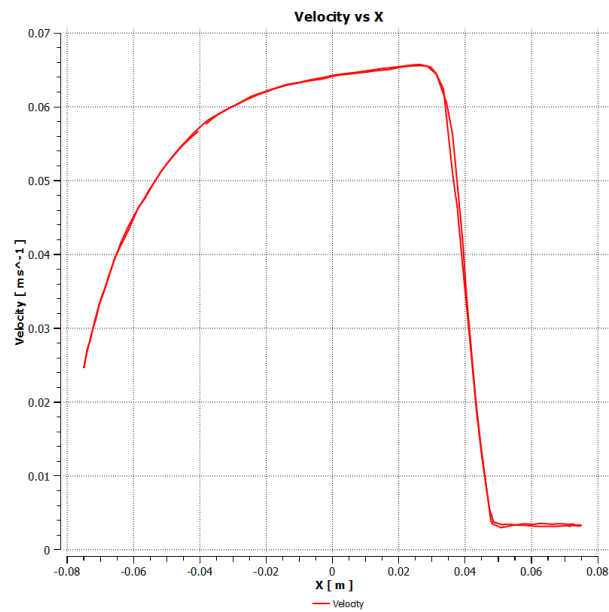


**Figure 11:** Velocity magnitude on surface of cylinder

The location where velocity suddenly drops has to be the separation point.

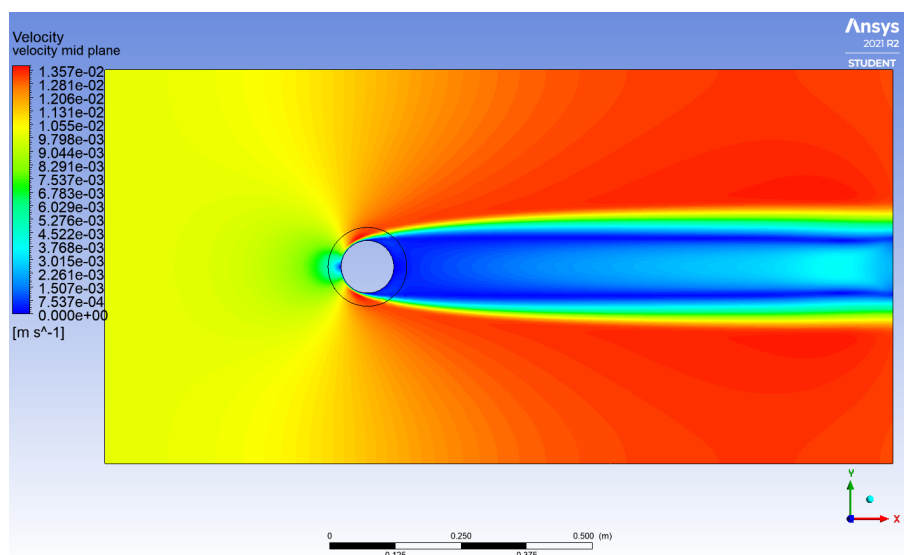


**Figure 12:** Velocity Contour

---

## 4.2 Case 2 and 3: With Lorentz Force

Two distinct cases were simulated. In both the cases a magnetic field of 5 Tesla is applied to only till a certain extent, this region (in green as visible in the image below) is another coaxial cylinder of 15 cm around the actual cylinder of 10 cm. But in one case the value of conductivity is just 10 S/m, corresponding to sea water conductivity, in another case the value of conductivity is just 50 S/m.

The interaction parameter is defined as

$$N = \frac{\sigma B^2 l}{\rho u_{\infty}}$$

For  $\sigma = 10$ ,  $N = 0.501$  and for  $\sigma = 50$ ,  $N = 2.505$

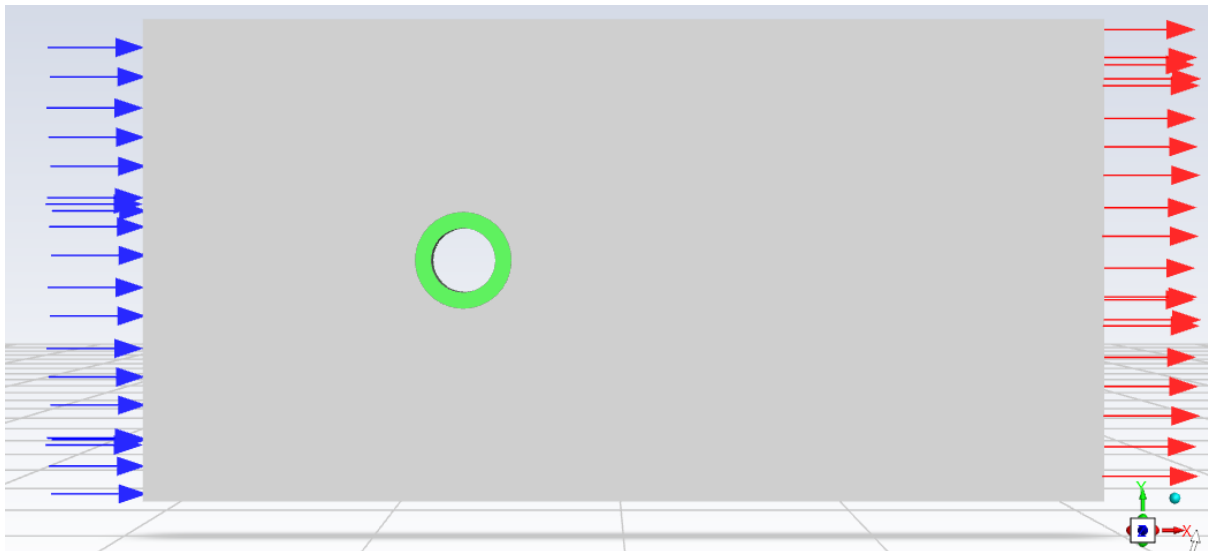


**Figure 13:** Magnetic Field Domain



---

### 4.2.1 Comparing Eddy Viscosity

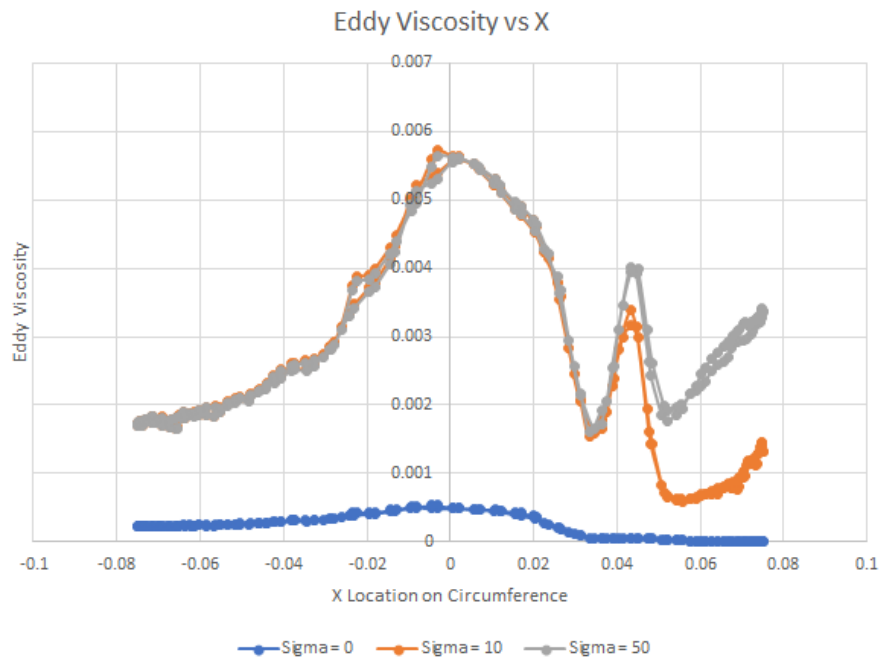


**Figure 14:** Eddy Viscosity Comparison

The eddy viscosity values without any magnetic field is significantly lower. This could be primarily because the magnetic field can create vorticity in the boundary layer. Here it seems there have been significant vorticity creation in the flow inside of the boundary layer.

---

### 4.2.2 Circumferential Velocity

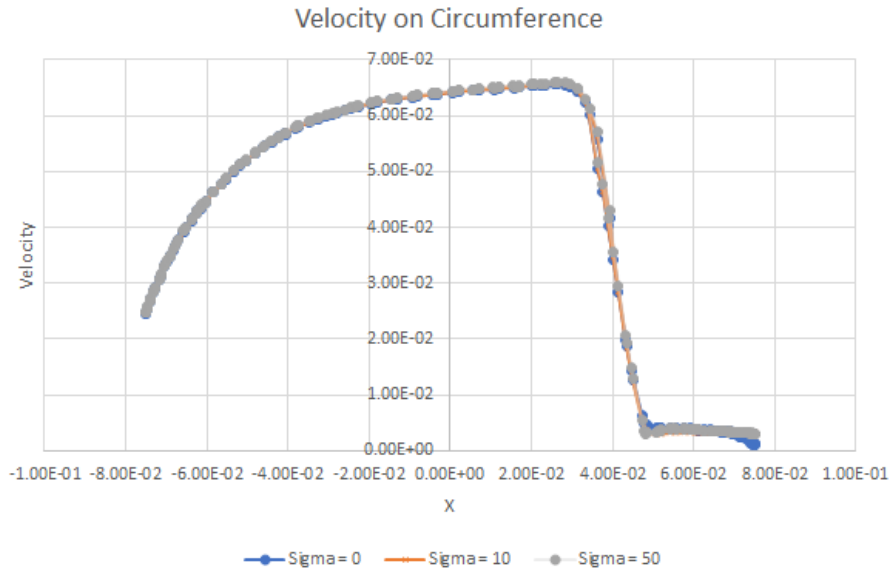


**Figure 15:** Velocity Comparison on outer cylinder

Another circle of 15 diameter cm is generated from the center of the cylinder and these profiles are plotted on this circle's circumference. This is done so as the boundary of the cylinder has no slip condition and magnitude of velocity goes to zero there.

### 4.2.3 Velocity Deficit

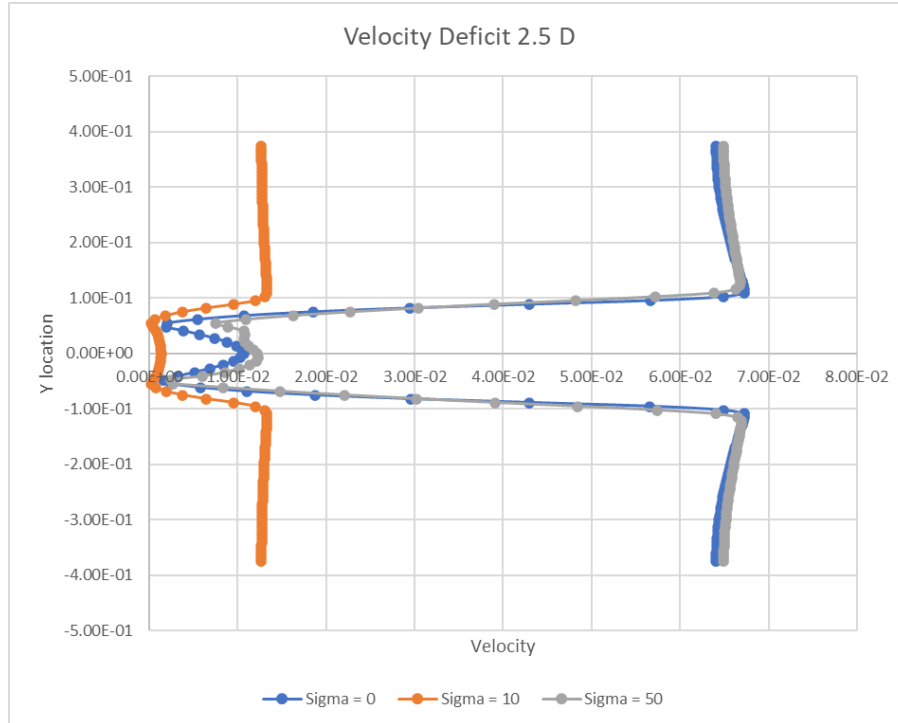


**Figure 16:** Velocity Comparison at 2.5D

Here the velocity is plotted along vertical lines at different x locations from the center of the cylinder, expressed in terms of a multiple of its diameter (the number in the title of the graph represents the distance of the vertical line from the center of the cylinder)

An interesting observation from the velocity graph is that the velocity recovery is smallest in the case where  $\sigma = 50$ . And the velocity recovery is highest in the case where there is a magnetic field with  $\sigma = 10$  (**please note that I mis-interpreted the data during the presentation, sincere apologies for that**). Velocity deficit is measured from the mean velocity of the flow at free-stream. Consider figure 18 for instance, the mean free-stream velocity for the case with  $\sigma = 10$  is about 1.32 cm/. And the maximum recovery is at the location  $y = 0$ , at which velocity is at about 0.23 cm/s, the difference being 1.09 cm/s. Whereas in the case with  $\sigma = 0$ , the mean free-stream velocity is about 6.5 cm/s, and at  $y = 0$ , the velocity is about 3 cm/s, difference being 3.5 cm/s. The difference falls to about 4.5 cm/s for the case with  $\sigma = 50$ . Hence the velocity deficit is the highest in  $\sigma = 50$ , then followed by  $\sigma = 0$  and finally lowest at  $\sigma = 10$ . Since drag can be directly integrated from velocity deficit, the drag has the same sequence as the velocity deficit.

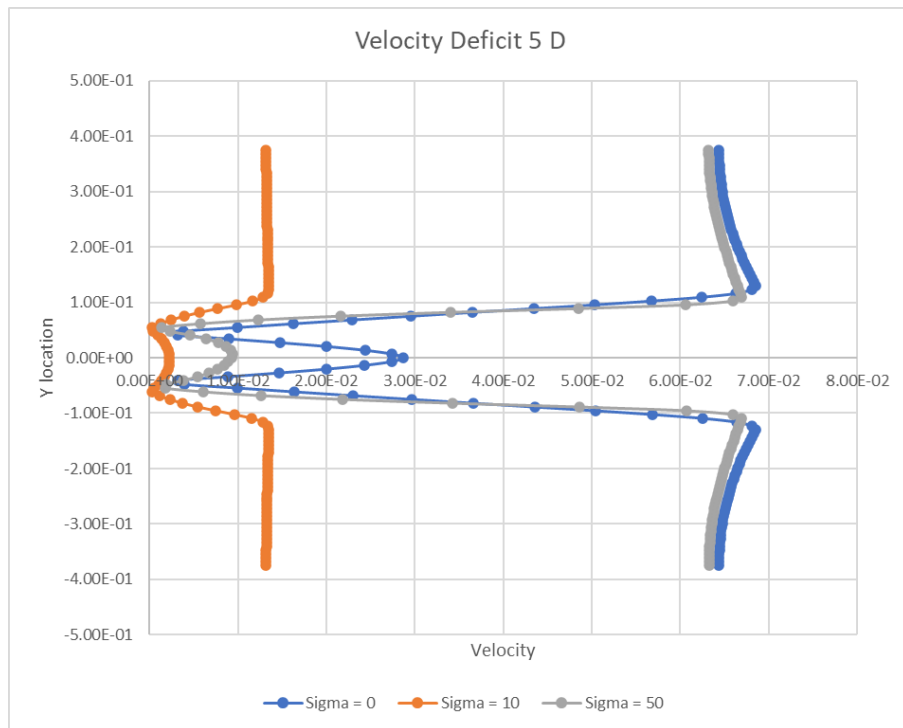


**Figure 17: Velocity Comparison at 5D**

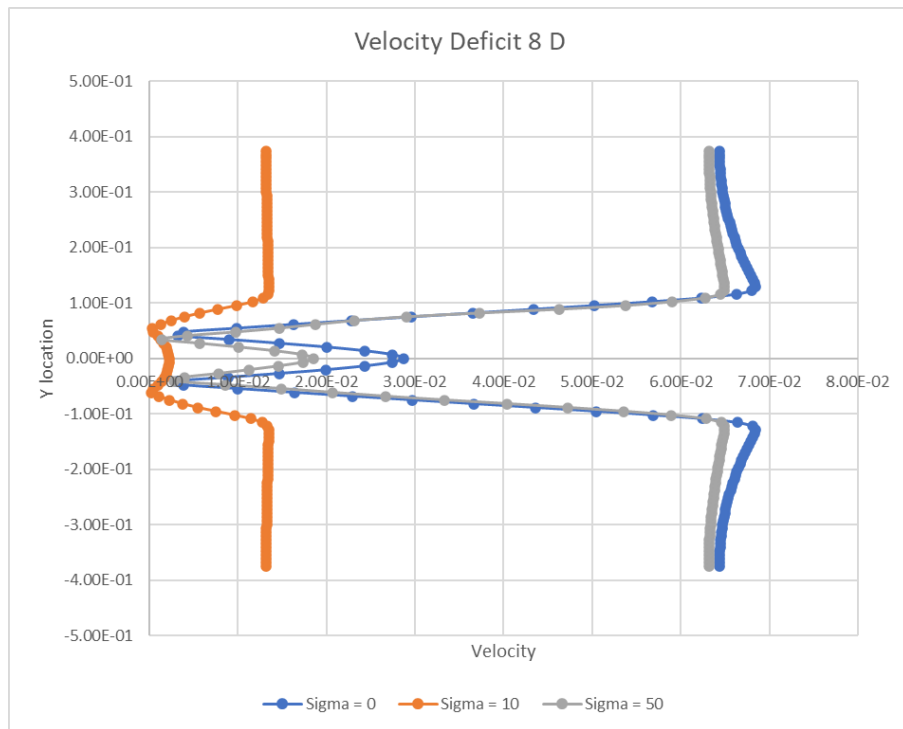


**Figure 18: Velocity Comparison at 8D**

The eddy viscosity comparison plot shows that with uniform magnetic field the eddy viscosity has increased in both the cases where magnetic field was applied.

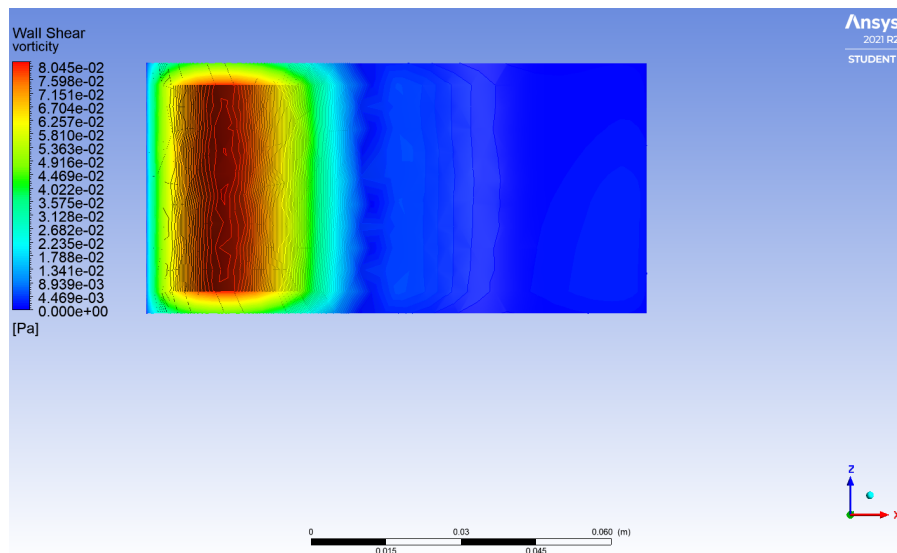


**Figure 19: Wall Shear Sigma = 0**

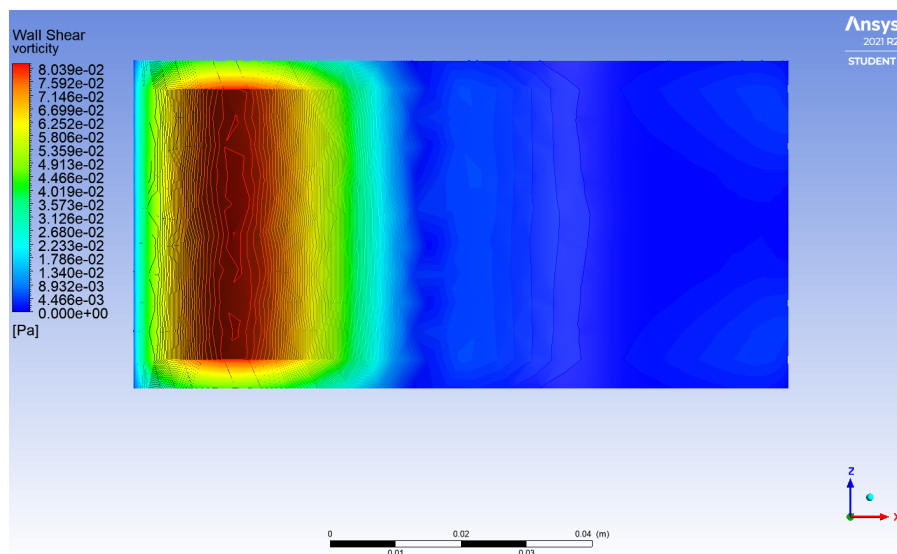


**Figure 20: wall shear contour Sigma = 10**

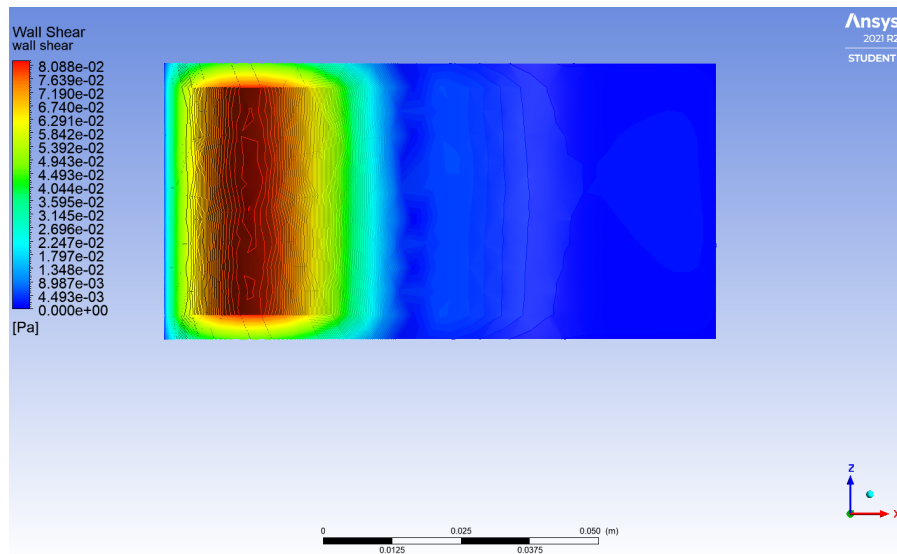


**Figure 21:** wall shear contour Sigma = 50

Comparing the above image with the wall shear stress for the previous case we can observe from the colour-bars that with MHD the wall shear has reduced only for the case  $\sigma = 10$ , this indicates that drag is indeed lower in the current case with a uniform magnetic field (only for  $\sigma = 10$ ). But in the case where  $\sigma = 50$ , the drag again has increased. The interaction parameter is crucial factor in deciding whether a given magnetic field will decrease or increase the drag. The interaction number for the case with  $\sigma = 10$  is about 0.5 and that for  $\sigma = 50$  is about 2.5. As per the study in reference [3] the drag reduction is highest for interaction number = 1, and for any value higher than 1 the drag value again increases, this conclusion is proved in the above study. The reasons for this behaviour is not clearly shown in this report, but one may expect the vorticity generated by the lorentz force to be the culprit.

### 4.3 Conclusion for Flow Over Cylinder

The turbulent drag does not always decrease with increase in Lorentz force, for interaction number less than 1 and reynolds number less than 5000 the turbulent drag decreases with increase in magnetic field. But after crossing interaction number of 1, drag again starts to increase due to high resistance of flow from the lorentz force opposing the mean flow. Hence the flow is unable to recover its mean velocity in the wake of the cylinder.

For practical applications MHD drag reduction methods are significantly inefficient due to the high load power required as mention in the introduction.

---

## 4.4 Results for Flow beyond a Backward Step

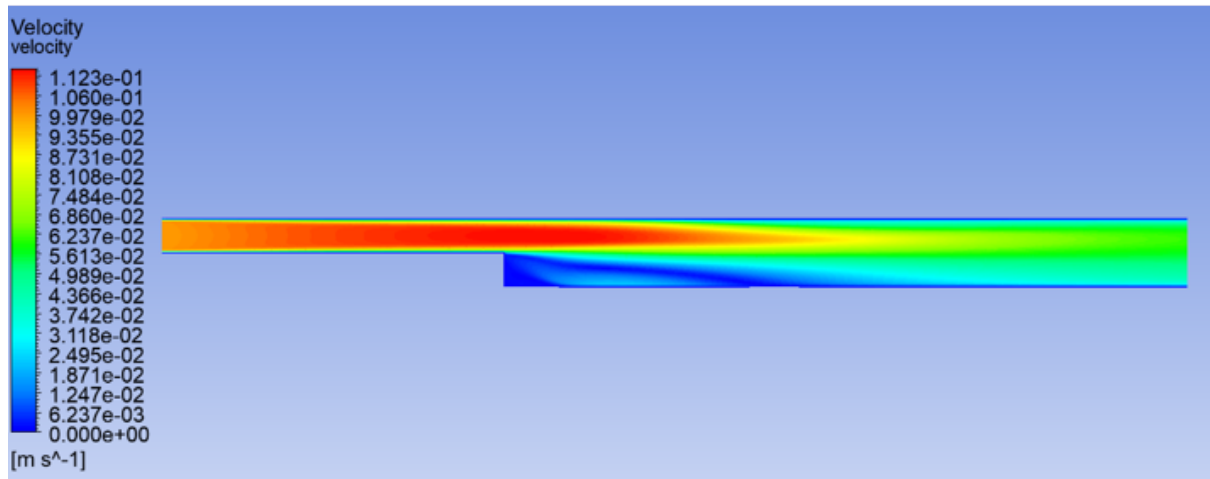


**Figure 22:** Velocity contour

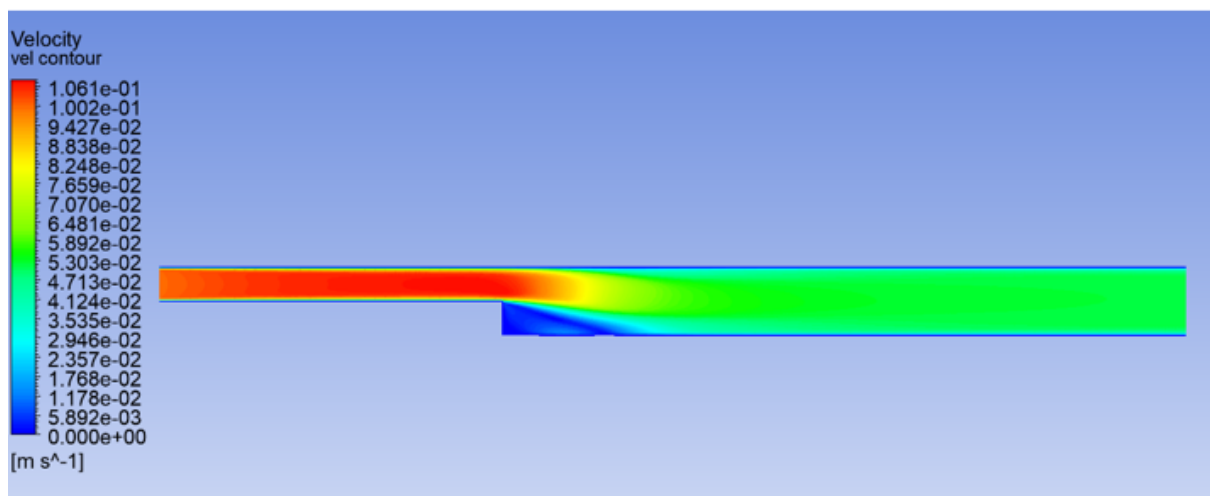


**Figure 23:** Velocity contour with B

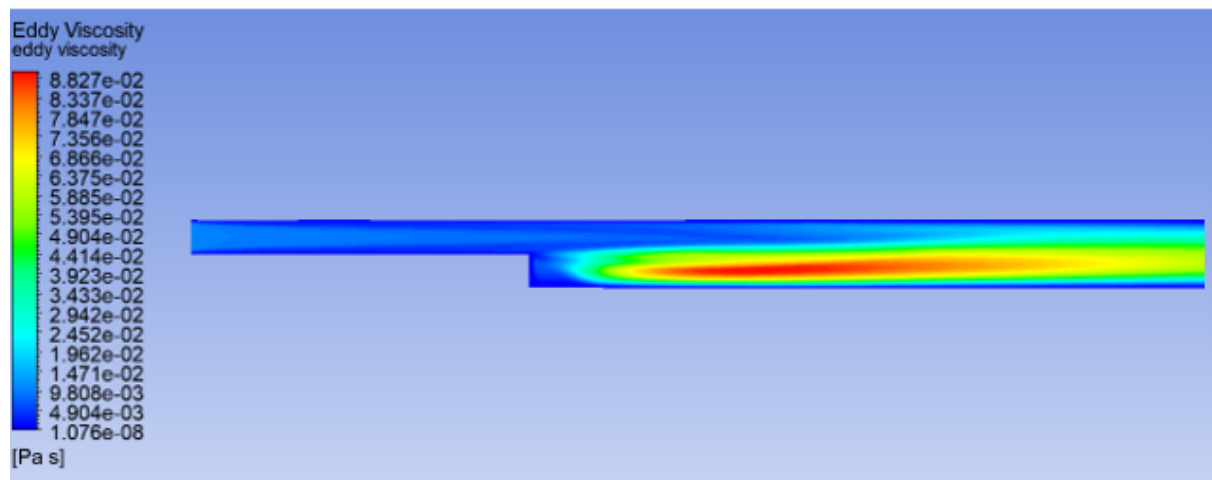


**Figure 24:** Eddy Viscosity without B

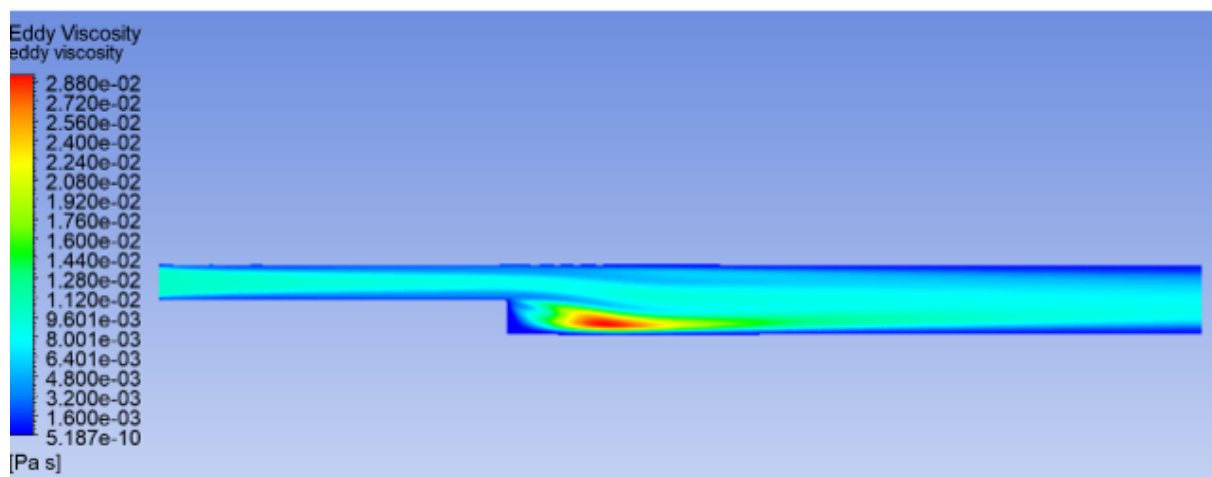


**Figure 25:** Eddy Viscosity with B



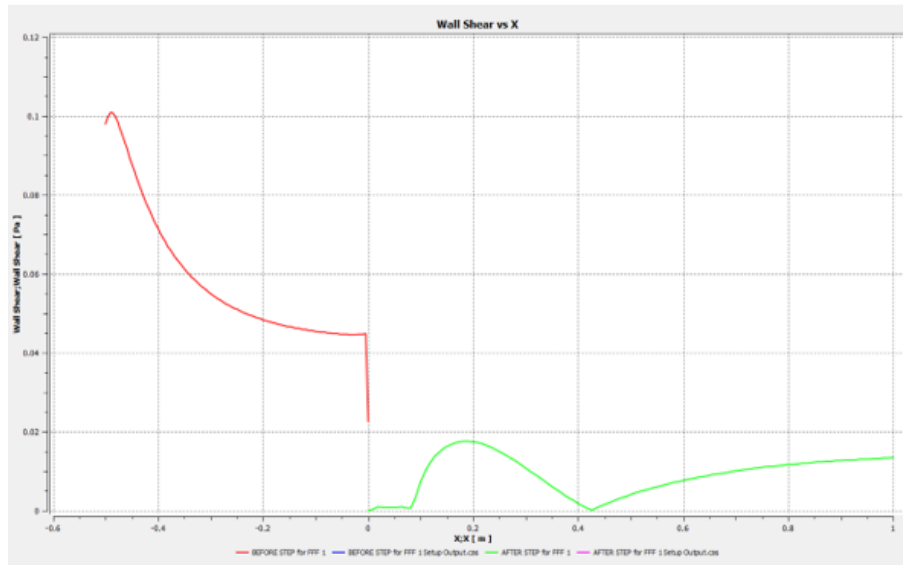


**Figure 26:** Eddy Viscosity  $\sigma = 0$

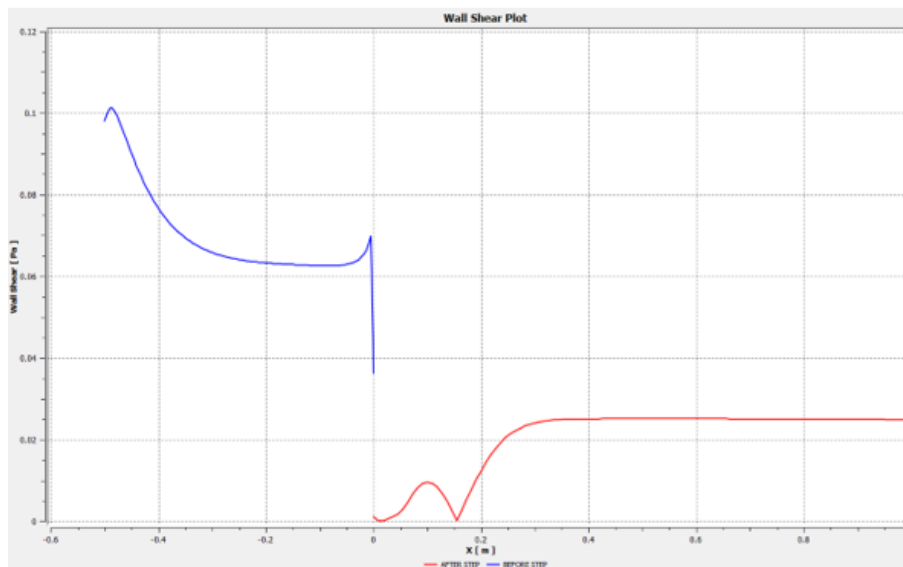


**Figure 27:** Eddy Viscosity  $\sigma = 10$

We can clearly see from the above plot that the separation point has indeed re-attached itself at a very shorter distance. One way to explain this is that the Lorenz force opposes the inertial force, hence decreases the momentum of the fluid in the X-direction; but the momentum in the Y direction stays unaffected, which can cause the fluid particle to reach the bottom wall in more or less the same time as it would have taken in the case where there is no B. Hence in the same time the distance travelled by the fluid parcel would be smaller in the X direction due to reduced momentum. This is a just a crude way to explain and understand this.

---

## 5 REFERENCES

- [1] Hiromichi Kobayashi "Large eddy simulation of magnetohydrodynamic turbulent duct flows", Fluids 20, 015102 (2008); Submitted: 02 August 2007 . Accepted: 24 November 2007 . Published Online: 25 January 2008
- [2] T. Albrecht, J. Stiller, H. Metzkes, T. Weier, and G. Gerbeth "Electromagnetic flow control in poor conductor", Eur. Phys. J. Special Topics 220, 275–285 (2013)
- [3] Leping Huang, Baochun Fan and Dongjie Mei, "Mechanism of drag reduction by spanwise oscillating Lorentz force in turbulent channel flow", Theoretical and Applied Mechanics
- [4] Christian Cierpka, Tom Weier and Gunter Gerbeth, "Synchronized force and particle image velocimetry measurements on a NACA 0015 in poststall under control of time periodic electromagnetic forcing", physics of Fluid
- [6] Pijush K. Kundu, Ira M. Cohen, David R Dowling - Fluid Mechanics-Academic Press (2015)
- [7] A. Fage, V.M. Falkner: An experimental determination of the intensity of friction on the surface of an airfoil